Interactions between Nucleotide Binding Sites on Chloroplast Coupling Factor 1 during ATP Hydrolysis†

Deborah Leckband‡ and Gordon G. Hammes*
Department of Chemistry, Cornell University, Ithaca, New York 14853
Received August 18, 1986; Revised Manuscript Received December 15, 1986

ABSTRACT: The initial hydrolysis of CaATP by chloroplast coupling factor 1 was studied with the quenched-flow method. The time course of hydrolysis can be described as a first-order conversion of the enzyme to an active form followed by steady-state formation of product. The rate constant for the first-order process is independent of substrate concentration but increases hyperbolically to a limiting value of 0.43 s^{-1} with increasing concentrations of free Ca^{2+}. A mechanism involving a Ca^{2+}-triggered conversion to an active form of the enzyme is consistent with the data. The steady-state rate varied sigmoidally with the CaATP concentration. Initial exchange of tightly bound ADP is complex: ~50% of the bound nucleotide is lost within 30 s, with complete exchange requiring several minutes. The first-order rate constant characterizing the rapid phase of the reaction increases hyperbolically to a limiting value of 0.26 s^{-1} as the concentration of CaATP is increased, indicating that the binding of CaATP to the enzyme promotes the exchange process. Modification of the quenched-flow apparatus permitted measurement of the rate of nucleotide exchange during steady-state catalysis. The value of the first-order rate constant characterizing this process is similar to the catalytic rate constant determined under identical conditions. When MgATP is tightly bound to the enzyme, none of the kinetic properties of the enzyme described above were significantly changed. The results obtained suggest a mechanism in which two sites on the enzyme participate in catalysis. Several possible mechanisms consistent with the data are discussed.

The chloroplast coupling factor catalyzes the reversible synthesis of adenosine 5′-triphosphate (ATP)[1] in photophosphorylation. Two distinct parts of the enzyme have been identified: a membrane-imbedded portion (CF_0) and a peripheral portion (CF_1), containing the substrate binding sites. The latter complex can be readily solubilized (Lien & Racker, 1971). Isolated CF_1 has a molecular weight of 400 000 (Moroney et al., 1983) and contains a latent ATPase activity [cf. McCarty and Moroney (1985)].

Nucleotide binding studies have revealed three nucleotide binding sites on both the membrane-bound (Harris & Slater, 1975; Cerione & Hammes, 1982) and soluble (Bruist & Hammes, 1981) forms of CF_1. One site on the isolated soluble enzyme, designated site 1, contains tightly bound ADP (Carlier & Hammes, 1979). This site exchanges readily with medium nucleotides during catalysis, although the rate of the initial release of ADP is much slower than the catalytic rate (Bruist & Hammes, 1982). The role of site 1 in catalysis is controversial. It clearly has ATPase (Bruist & Hammes, 1981) and ATP synthesis (Feldman & Sigman, 1982) capabilities. However, whether it plays primarily a regulatory (Bar-Zvi & Shavit, 1982; Bruist & Hammes, 1982) or a catalytic (Wu & Boyer, 1986) function has been debated. A second site binds ATP tightly in the presence of magnesium (site 2). This tightly bound nucleotide is not removed by dialysis or during catalytic turnover (Bruist & Hammes, 1981, 1982). The third site (site 3) binds nucleotides reversibly in the presence or absence of metals and serves a primary catalytic function.

In this work, the kinetic behavior of the individual sites has been examined during the intial stages of CaATP hydrolysis by use of the quenched-flow method. Both the initial rate of the nucleotide release from site 1 and the steady-state rate of nucleotide incorporation at this site have been measured. Modification of the quenched-flow apparatus permitted the steady-state measurements to be made. The effects of MgATP bound to site 2 on nucleotide dissociation from site 1, catalysis, and ADP inhibition of catalysis were examined. The results obtained suggest that both site 1 and site 3 are catalytic sites, whereas the role of site 2 could not be ascertained.

Materials and Methods

Chemicals. ATP (vanadium free), ADP, Tris, creatine kinase, phosphocreatine, and NADH were from Sigma Chemical Co. Radioactive [^{3}H]ATP was from ICN, and [γ-^{32}P]ATP and [α-^{32}P]ATP were from Amersham. Nucleotides were purified as described (Bruist & Hammes, 1981). All other chemicals were high-quality commercial grades. Solutions were prepared with deionized, distilled water.

Enzyme. CF_1 was prepared as described elsewhere (Lien & Racker, 1971; Binder et al., 1978). Protein used in these studies had a 305:340-nm fluorescence ratio (280-nm excitation) greater than 1.7 and catalyzed CaATP hydrolysis at a rate of 20–30 μmol mg^{-1} min^{-1} in 5 mM $CaCl_2$, 5 mM ATP, 40 mM Tris, and 1 mM EDTA (pH 8.0) when assayed for 5 min at 37 °C. CF_1 was activated by heating the enzyme at 60 °C for 4 min in the presence of 40 mM ATP, 10 mM dithiothreitol, 20 mM Tris, and 1 mM EDTA (pH 8.0) (Farron & Racker, 1970). Enzyme was stored as an ammonium sulfate precipitate at 4 °C for not more than 4 weeks. Dissociable nucleotides were removed by passage of the enzyme through 3.0-mL Sephadex G-50 centrifuge columns (Penefsky, 1977). Enzyme solutions were concentrated by using a Centricon Concentrator (M_r 10 000 cutoff, Amicon) or by precipitation with saturated ammonium sulfate followed

† This work was supported by a grant from the National Institutes of Health (GM 13292).
‡ National Institutes of Health Predoctoral Trainee (GM 07273).

[1] Abbreviations: CF_1, chloroplast coupling factor 1; ATP, adenosine 5′-triphosphate; ADP, adenosine 5′-diphosphate; EDTA, ethylenediaminetetraacetic acid; Tris, tris(hydroxymethyl)aminomethane; NADH, reduced nicotinamide adenine dinucleotide.

0006-2960/87/0426-2306$01.50/0

by centrifugation and resuspension in a minimal amount of buffer. Heat-activated enzyme could be stored as an ammonium sulfate precipitate at 4 °C for up to 48 h with no change in kinetic behavior. Enzyme concentrations were determined with an extinction coefficient of 0.483 mL/(mg·cm) at 277 nm (Bruist & Hammes, 1981) and a molecular weight of 400 000 (Moroney et al., 1983). The adenine nucleotide concentrations were determined by absorbance measurements with an extinction coefficient of 15.4 mM^{-1} cm^{-1} at 259 nm, pH 8.0 (Bock et al., 1956).

The nucleotide binding site containing tightly bound ADP (site 1) was labeled with radioactive ADP by incubating heat-activated CF_1 with 0.2 mM [^{3}H]ATP (10^{11} cpm/mmol) and 0.5 mM $CaCl_2$ in 40 mM Tris, pH 8.0, for 15 min at room temperature, followed by passage through centrifuge columns equilibrated with 50 mM NaCl, 20 mM Tris, and 0.5 mM EDTA at pH 8.0. The stoichiometry of bound nucleotide was determined by measuring the amount of radioactivity in an aliquot with a Beckman LS200 scintillation counter and determining the protein concentration by absorbance measurements, after correcting for light scattering. Typical stoichiometries ranged from 0.8 to 1.1 [^{3}H]ADP/CF_1.

The nucleotide binding site that binds MgATP very tightly (site 2) was labeled by incubation of heat-activated enzyme with 0.2 mM [γ-^{32}P]ATP (10^{11} cpm/mmol) and 0.5 mM $MgCl_2$ for 1 min in 40 mM Tris, pH 8.0, at room temperature, followed by passage through two consecutive centrifuge columns equilibrated with 20 mM Tris and 10 mM EDTA (pH 8.0). The labeled enzyme was incubated in this buffer for 2 h before the excess EDTA was removed by passage through a PD-10 column (Pharmacia) equilibrated with the same NaCl–Tris–EDTA buffer as above. After the initial 60-s incubation, a stoichiometry of 1.5–1.8 ^{32}P/CF_1 was found. Passage through a second column a few minutes later reduced the stoichiometry to 0.9–1.1 [^{32}P]ATP/CF_1; the stoichiometry was not reduced further by use of additional columns or by incubation with CaATP.

When both site 1 and site 2 were labeled simultaneously, the enzyme was first incubated with [γ-^{32}P]MgATP as described above. Dissociable nucleotides and [^{32}P]P_i were removed with two centrifuge columns, and the stoichiometry was determined. The enzyme was then reacted with [^{3}H]CaATP as described above and passed through two centrifuge columns, and the stoichiometry of bound ^{32}P and ^{3}H was determined by use of two channels on the scintillation counter. When this procedure was used, the amount of ^{32}P lost in the second labeling step was negligible.

In all cases, the labeled enzyme was incubated in 50 mM NaCl, 20 mM Tris, and 0.5 mM EDTA (pH 8.0) for at least 2 h prior to the quenched-flow experiments.

Nucleotide Release Assays. The kinetics of release of enzyme-bound nucleotides was followed with the nitrocellulose filter assay (Bruist & Hammes, 1982). Nitrocellulose filters (BA83, 0.2 μm, and 25 mm; Schleicher & Schuell) were presoaked in 20 mM Tris (pH 8.0) for at least 12 h before use. Solution volumes containing 5–12 μg of protein were applied to a filter mounted on a filter holder assembly (BG27; Schleicher & Schuell). Solutions were allowed to absorb slowly, after which the filter was washed with three 0.25-mL aliquots of soaking buffer under vigorous aspiration. Filters were then placed in 1.0 mL of methanol followed by 10 mL of ACS scintillation cocktail. In all nitrocellulose assays, the time elapsed during filtration of samples is negligible compared to the exchange rate of the bound nucleotides; i.e., the loss of label during filtration is negligible.

The effect of exogenous ADP on nucleotide release from site 1 was studied by using creatine kinase as an ADP scavenger. Release of nucleotides was followed as described above in the presence and absence of creatine phosphate under the conditions described by Wu and Boyer (1986) for ATP regeneration. The time course of the reaction was determined by removal of 0.3-mL aliquots of solution at various time intervals; the aliquots were then passed through two consecutive centrifuge columns, and the amount of radioactive label bound per milligram of protein was determined by scintillation counting and absorbance measurements. Parallel experiments were carried out with the nitrocellulose binding assay.

Steady-State Kinetics. The steady-state rate of CaATP hydrolysis by CF_1 was measured in 50 mM NaCl, 20 mM Tris, and 0.5 mM EDTA, pH 8.0, and varying amounts of $CaCl_2$ and ATP at 37 °C. The concentration of free Ca^{2+} was fixed at 5.0 mM. Each 1.0-mL reaction mixture was quenched after 60 s with 0.1 mL of 50% trichloroacetic acid. The [^{32}P]P_i liberated was determined by mixing 0.5 mL of the quenched reaction mixture with 0.5 mL of 16% ammonium molybdate in 10 N HCl followed by extraction with 2.0 mL of 1:1 isobutyl alcohol–benzene (Avron, 1960). The radioactivity in the upper organic layer was measured, after centrifugation in a bench-top centrifuge, to determine the amount of [^{32}P]P_i. Inhibition of the enzyme activity by ADP was examined in the presence of 200 μM ADP. The concentration of $CaCl_2$ for these measurements was equal to the sum of ATP and ADP concentrations plus 5.0 mM. The amount of enzyme added to each solution was adjusted to limit the hydrolysis to less than 5% of the amount of CaATP.

Quenched-Flow Measurements. The quenched-flow apparatus used has been described (Cognet & Hammes, 1983). The instrument dead time was determined to be 10 ms under the experimental conditions used by monitoring the rate of hydrolysis of 0.4 mM dinitrophenol acetate in 0.2–0.04 M NaOH at 20 °C. The reaction was quenched with 1.0 M HCl and the extent of reaction determined by measurement of the absorbance at 320 nm (Cash & Hess, 1981). The kinetics of ATP hydrolysis was studied at 20 °C in 50 mM NaCl, 20 mM Tris, 0.5 mM EDTA, pH 8.0, and varying concentrations of $CaCl_2$ and ATP. Free calcium concentration was maintained at 1.0 mM, unless otherwise indicated. A dissociation constant for CaATP formation of $10^{-3.74}$ M was used to calculate the concentration of free Ca^{2+} (Khan & Martell, 1962). The quenching buffer consisted of 200 mM EDTA and 20 mM Tris at pH 8.0. The initial rate experiments were carried out with the instrument operating in the pulse–pulse mode, with incubation times ranging from 0.4 to 45 s. The extent of calcium-dependent [γ-^{32}P]ATP hydrolysis was assayed with a charcoal extraction method (Schinkel & Hammes, 1986).

The effect of the quenched-flow measurements on the enzyme activity was assessed by passing heat-activated enzyme through the longest tubing at the maximum flow rate. The enzyme was then collected and assayed. No detectable loss of activity was found.

The steady-state turnover rate at site 1 was examined with the quenched-flow apparatus modified as shown in Figure 1. In this assembly, the first incubation with unlabeled substrate is for the duration of time required to exchange bound nucleotide from site 1 to a defined extent, as determined by control experiments. The first incubation is followed by a radioactive substrate chase in which the second incubation period, with labeled substrate, is varied by changing the length of the incubation tubing. Incubation times achieved by varying the length of incubation tubing ranged from 150 to 500 ms.

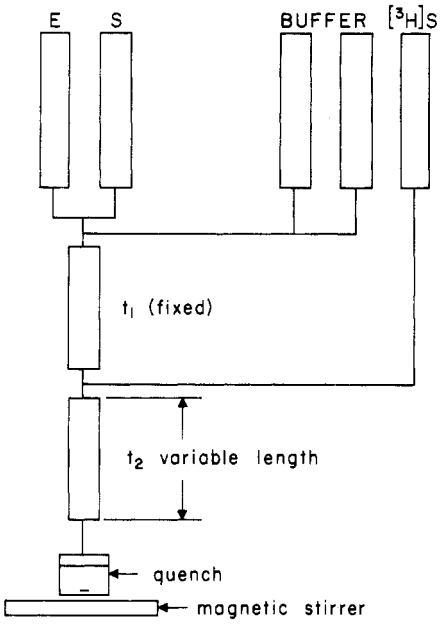

FIGURE 1: Modified quenched-flow apparatus. Two incubation periods are possible for two different combinations of reactants, and the quenching of the reaction is carried out in the flask at the bottom of the figure.

Samples were quenched by eluting the solution into a collecting vessel containing 0.2 mL of quenching buffer. For incubation times exceeding 500 ms, the enzyme–substrate mixture was eluted into the collecting vessel and quenched manually. The collecting vessel was mounted on a vortex to ensure rapid mixing. Immediately after quenching, 100 μL of solution was filtered and processed as above. The dead time for the instrument in this arrangement was found to be about 100 ms.

RESULTS

The initial hydrolysis of ATP by CF_1 was studied with the quenched-flow method in 50 mM NaCl, 20 mM Tris, and 0.5 mM EDTA (pH 8.0) at 20 °C. The range of CaATP concentrations was 10–120 μM and the range of CF_1 concentrations 0.1–0.75 mg/mL, with the concentration of free Ca^{2+} fixed at 1.0 mM. A typical time course is shown in Figure 2. In all cases, the time course analyzed did not extend beyond a few turnovers per enzyme molecule. This restricted the upper range of CaATP concentrations due to the difficulty in precisely measuring small changes in the ATP concentration at high ATP concentrations. The time courses are characterized by a lag followed by a linear loss of ATP with time. A simple mechanism consistent with the data is

$$E_i \xrightarrow{k} E_a \quad (1)$$

$$(E_a + S \rightleftharpoons E_aS) \rightarrow E_a + P \quad (2)$$

where k is the rate constant characterizing the interconversion of an inactive form of the enzyme, E_i, to an active form, E_a. The second step depicts the combination of enzyme and substrate, S, to give a complex followed by the release of products, P. At this stage of the analysis, the exact mechanism need not be specified other than to stipulate it is some form of a Michaelis–Menten mechanism, with or without cooperativity. For this general mechanism, the rate of formation of product is

$$d[P]/dt = \beta[E_a]_T \quad (3)$$

where β is the initial steady-state velocity divided by the total concentration of active enzyme, $[E_a]_T$. From eq 1

$$[E_a]_T = [E_0](1 - e^{-kt}) \quad (4)$$

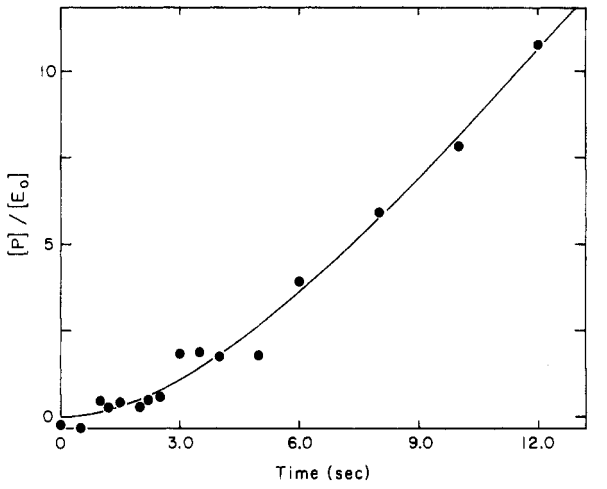

FIGURE 2: Representative time course for the hydrolysis of CaATP obtained by mixing equal volumes of heat-activated CF_1 and substrate. The final concentrations were 1.0 μM CF_1, 1.0 mM free Ca^{2+}, and 75 μM CaATP in 50 mM NaCl, 20 mM Tris, and 0.5 mM EDTA, pH 8.0, at 20 °C. The specific activity of the CF_1 was 24 μmol/(mg·min). The line was calculated with eq 5 and the best-fit parameters $\beta = 1.6 \pm 0.5$ s^{-1} and $k = 0.16 \pm 0.08$ s^{-1}.

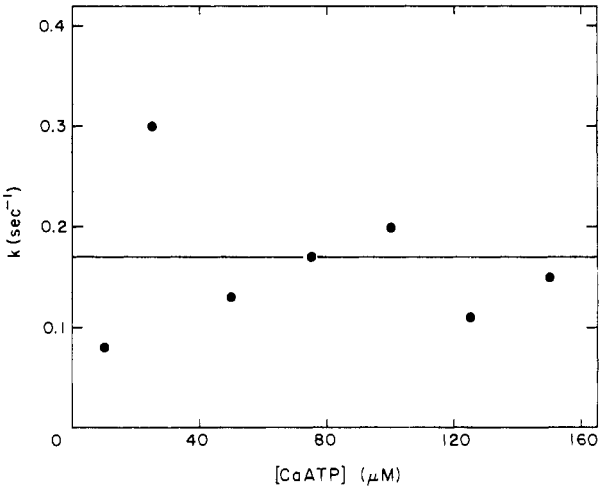

FIGURE 3: Plot of the rate constant, k, characterizing the conversion of inactive to active CF_1 vs. the CaATP concentration. Experimental conditions were as given in the legend to Figure 2, except for varying the concentration of CaATP. The line is the weighted average value of k, 0.17 ± 0.06 s^{-1}.

where $[E_0]$ is the total enzyme concentration. Substitution of eq 4 into eq 3 and integration give

$$[P]/[E_0] = \beta t + (\beta/k)(e^{-kt} - 1) \quad (5)$$

Equation 5 was found to fit the data well; the curve in Figure 2 represents a nonlinear least-squares fit of the data to eq 5.

As illustrated in Figure 3, the rate constant k shows no systematic dependence on the concentration of CaATP over the range 10–150 μM. The weighted average value of k is 0.17 ± 0.06 s^{-1}. (The weighting factor is the reciprocal of the square of the standard deviation obtained from the fitting of the data to eq 5.) However, the value of k depends significantly on the concentration of free Ca^{2+}. Figure 4 shows the variation of k with free Ca^{2+} with [CaATP] = 75 μM. If these data are analyzed with the assumption of a hyperbolic binding isotherm for free Ca^{2+}

$$k = \frac{k_m}{1 + K/[Ca^{2+}]} \quad (6)$$

Here k_m is the maximum rate constant, and K is the equilibrium dissociation constant for the binding of Ca^{2+} to the

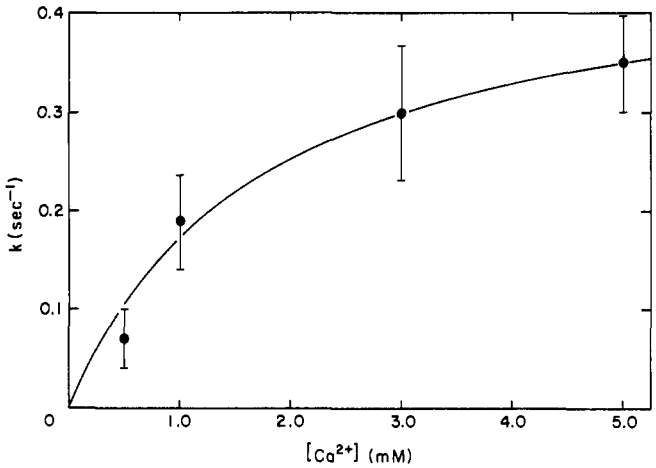

FIGURE 4: Plot of the rate constant, k, for the conversion of inactive to active CF_1 vs. the free Ca^{2+} concentration. Experiments were carried out in 75 μM CaATP, 50 mM NaCl, 20 mM Tris, and 0.5 mM EDTA, pH 8.0, at 20 °C, with varying concentrations of free Ca^{2+}. Each point represents the average of two to five experiments, and error bars represent one standard deviation. The solid line was calculated with eq 6 and the best-fit parameters $k_m = 0.43 \pm 0.03$ and $K = 1.6 \pm 0.2$ mM.

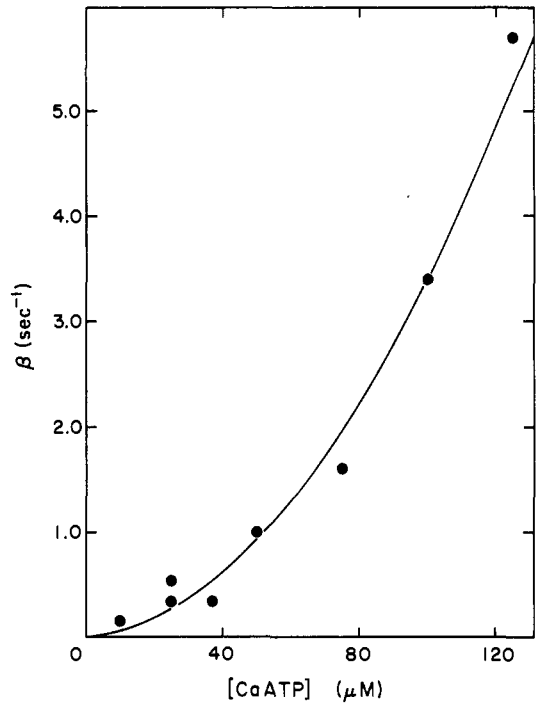

FIGURE 5: Plot of β vs. the CaATP concentration. Experimental conditions were as given in the legend to Figure 2, except for varying the concentration of CaATP. The curve was calculated with eq 9 and the best-fit parameters $A_0 = (3.0 \pm 0.4) \times 10^{-3}$ μM^{-1} s^{-1} and $B_0 = (3.1 \pm 0.5) \times 10^{-4}$ μM^{-2} s^{-1}.

enzyme. A weighted nonlinear least-squares treatment of the data gives $k_m = 0.43 \pm 0.03$ s^{-1} and $K = 1.6 \pm 0.2$ mM.

The dependence of β on the concentration of CaATP is illustrated in Figure 5. These data were obtained with the same preparation of enzyme on the same day to avoid variations in the specific activity of the enzyme. The data in Figure 5 clearly do not describe a hyperbolic isotherm, consistent with an earlier investigation of the steady-state kinetics (Bruist & Hammes, 1982). Possible mechanisms in accord with these results are discussed later.

A typical time course for the release of radioactive ADP bound to site 1 during ATP hydrolysis is presented in Figure 6. The conditions used to study this nucleotide release were

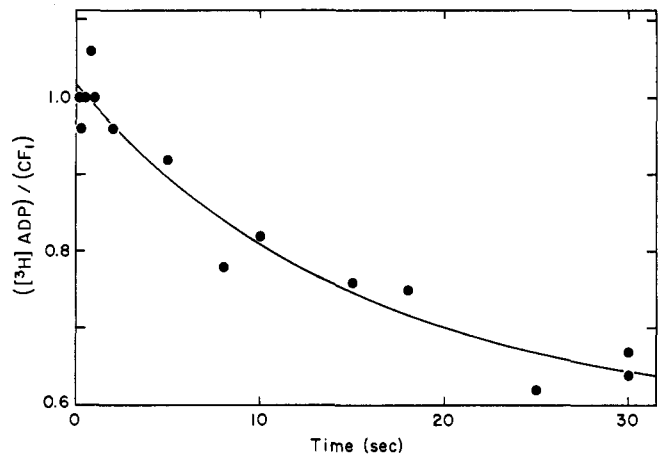

FIGURE 6: Typical plot of the stoichiometry of radioactive ADP in site 1 vs. time during CaATP hydrolysis. The experiment was carried out in 50 mM NaCl, 20 mM Tris, 0.5 mM EDTA, pH 8.0, 1.0 mM free Ca^{2+}, and 100 μM CaATP at 20 °C. The line was calculated with eq 7 and the best-fit parameters $[ADP_i]/[E_0] = 1.02 \pm 0.07$, $k_e = 0.07 \pm 0.03$ s^{-1}, and constant $= 0.58 \pm 0.07$.

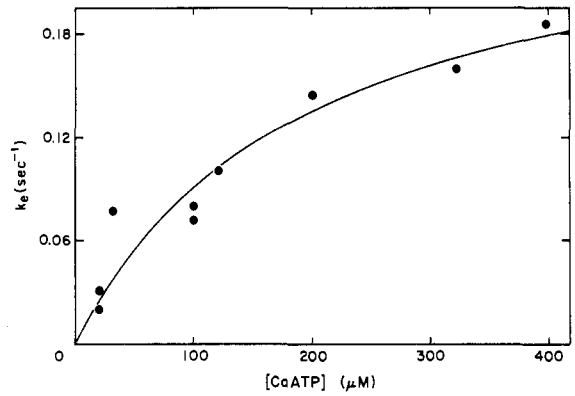

FIGURE 7: Plot of the rate constant for the initial exchange of [^{3}H]ADP from site 1, k_e, vs. the CaATP concentration. Experimental conditions were as given in the legend to Figure 6, with varying CaATP concentrations. The solid line was calculated with eq 6 and the best-fit parameters $k_m = 0.26 \pm 0.04$ s^{-1} and $K = 191 \pm 68$ μM.

identical with those used for the study of ATP hydrolysis in the quenched-flow experiments. Approximately 40–50% of the nucleotide is lost within the first 20 s for the data shown. Complete loss of nucleotide takes about 15 min. The fraction of nucleotide that rapidly exchanges does not depend significantly on the concentration of CaATP. The rapid phase of the loss of nucleotide is well described by a first-order rate equation:

$$[ADP]/[E_0] = [ADP_i]/[E_0] \exp(-k_e t) + \text{constant} \quad (7)$$

where [ADP] is the concentration of bound ADP, the subscript i represents the initial value, and k_e is the first-order rate constant. The curve in Figure 6 has been obtained by a nonlinear least-squares fit of the data to eq 7. The dependence of k_e on the concentration of CaATP is shown in Figure 7. The data can be described by a hyperbolic isotherm (eq 6 with CaATP substituted for Ca^{2+}). The best-fit parameters are $k_m = 0.26 \pm 0.04$ s^{-1} and $K = 191 \pm 68$ μM; the curve in Figure 7 has been calculated with these parameters and eq 6. The possibility exists that the amount of ADP formed by hydrolysis of ATP influences the rate and extent of ADP dissociation from site 1. However, if creatine kinase is used as an ADP scavenger, the rate and amount of rapidly exchanged ADP are not significantly changed.

The initial release of ADP bound at site 1 may be characterized by a different rate than during steady-state hydrolysis

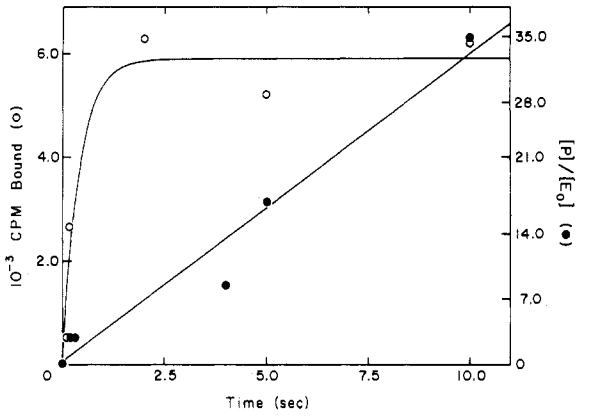

FIGURE 8: Representative plots of the time courses of steady-state ADP incorporation into site 1 (○) and CaATP hydrolysis (●). Experiments were carried out at 20 °C in 50 mM NaCl, 20 mM Tris, 0.5 mM EDTA, pH 8.0, 1.0 mM $CaCl_2$, 50 μM CaATP in the first incubation, and 120 μM [^{3}H]CaATP or [γ-^{32}P]CaATP in the second incubation. The curve for ADP incorporation was calculated with eq 8 and the best-fit parameters $A(\infty)$ = 5900 ± 500 cpm and k_e = 2 ± 1 s^{-1}. The line for ATP hydrolysis was fit to $[P]/[E_0] = \beta t$; the value of β found was 3.2 ± 0.3 s^{-1}.

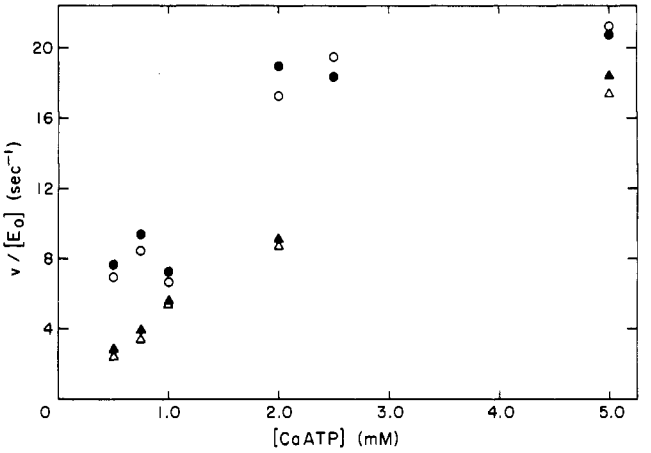

FIGURE 9: Plot of the initial steady-state velocity of CaATP hydrolysis divided by the total enzyme concentration, $v/[E_0]$, vs. the CaATP concentration. The experiments were carried out in 50 mM NaCl, 20 mM Tris, and 0.5 mM EDTA, pH 8.0, with 5.0 mM free Ca^{2+} at 37 °C, with (○, △) and without (●, ▲) MgATP at site 2 and with (△, ▲) and without (○, ●) 200 μM ADP.

of ATP. The modified quenched-flow method (Figure 1) was used to explore this possibility. The enzyme is first incubated with CaATP for a time, t_1, long enough to allow >90% of the bound ADP to be exchanged from the rapidly exchanging population, as determined in a separate experiment. Rapid addition of radioactively labeled substrate, [^{3}H]CaATP, is followed by a second incubation period, t_2. The rate of incorporation of radioactive label into site 1 is followed by rapid quenching of CaATP hydrolysis at various times during the second incubation period. A typical time course for incorporation is shown in Figure 8. Here t_1 = 15 s, [CaATP] = 120 μM, and [Ca^{2+}] = 1.0 mM. The incorporation of label follows a first-order rate equation:

$$A(t) = A(\infty)[1 - \exp(-k_e t)] \quad (8)$$

where $A(t)$ is the amount of radioactivity bound to the enzyme at time t. A nonlinear least-squares analysis of the data gives k_e = 2 ± 1 s^{-1}. The initial steady-state rate, v, also was determined during the second incubation period. The time course does not show a lag (Figure 8), and the value of $v/[E_0]$ determined from the slope of the line in Figure 8 is 3.2 ± 0.3 s^{-1}. These results indicate that the rate of loss of the first ADP from site 1 is slower than during steady-state ATP hydrolysis. Furthermore, during steady-state ATP hydrolysis, the rate constant characterizing nucleotide incorporation into site 1 is comparable to the catalytic rate constant, $v/[E_0]$. Similar results were obtained in several different experiments.

The function of the site that binds MgATP tightly also was examined (site 2). In agreement with earlier work (Bruist & Hammes, 1982), radioactive bound MgATP is not released from site 2 in any significant amount (<10%) during steady-state hydrolysis of ATP. This is not due to an inhibitory effect of Mg^{2+} on hydrolysis since the same result was obtained when the ATP hydrolysis was done after incubating the enzyme with tightly bound MgATP at site 2 in 20 mM Tris and 10 mM EDTA (pH 8.0) for 2 h. Furthermore, neither the rate of ATP hydrolysis nor the initial rate of release of ADP from site 1 was altered by the binding of MgATP at site 2. Finally, the noncompetitive inhibition of ATP hydrolysis by ADP was identical with or without MgATP at site 2 (Figure 9). These results indicate that site 2 does not serve as a catalytic site for ATP hydrolysis nor does it play an obvious regulatory role.

DISCUSSION

The time course of the initial rate of CaATP hydrolysis by CF_1 is consistent with a relatively simple mechanism (eq 1 and 2). The initial process is the conversion from an inactive form of the enzyme to an active form triggered by the binding of Ca^{2+} to the enzyme. This is consistent with the dependence of the rate constant for the interconversion on the concentration of free Ca^{2+} (Figure 4). The rate constant does not depend significantly on the concentration of CaATP over the concentration range studied (Figure 2). (Because changes in the concentration of free calcium parallel changes in the [CaATP]:[ATP] ratio, the possibility cannot be excluded that this ratio is of significance in the interconversion.) These results differ from those in an earlier study where the pre-steady-state induction period was found to depend on the concentration of CaATP, rather than free metal (Carmelli, 1979). Recent studies on the membrane-bound system have implicated free Mg^{2+} as a regulator of ATPase activity (Shahak, 1986). In those studies, free metal was found to enhance the rate of ATPase activation under energized conditions. Although the activation by Mg^{2+} was relatively slow (minutes), the regulatory function of free metal was clearly demonstrated.

The initial release of tightly bound ADP from the enzyme is slow compared with the rate of ATP hydrolysis: the two rate constants differ by at least an order of magnitude. Moreover, the process is complex: part of the population exchanges rapidly (seconds), whereas the remaining population exchanges much more slowly (minutes). The relative amounts of the two (or more) populations are not affected by the levels of ATP or ADP present. Most likely some heterogeneity in the population of enzyme conformations exists. The rate constant for the rapidly exchanging population (~50%) increases with increasing CaATP concentration and reaches a maximum value of 0.26 ± 0.04 s^{-1} (Figure 7). This maximum value is similar to the rate constant characterizing the interconversion of inactive to active enzyme (0.17 ± 0.06 s^{-1}). A simple explanation for these findings is that the active ATPase can undergo rapid exchange of tightly bound nucleotide if CaATP is bound at a second site on the enzyme, whereas exchange is very much slower for the inactive form of the enzyme. Studies with the membrane-bound system revealed a rapid loss of tightly bound nucleotides upon illumination of thylakoids (Strotmann & Bickel-Sandkötter, 1977). Also, the

release of tightly bound nucleotide has been found to parallel ATPase activation (Schumann & Strotmann, 1981). The data presented here suggest that activation precedes nucleotide release, rather than results from nucleotide loss. Since the presence of enzyme-bound MgATP at site 2 has no effect on the exchange process, presumably CaATP binding at site 3 is required for the rapid phase of the initial exchange reaction. However, the involvement of other sites not yet characterized cannot be excluded. The dependence of the rate constant for the exchange reaction on the concentration of CaATP is hyperbolic, consistent with the participation of a single binding site.

Perhaps the most significant finding in this work is that under identical conditions, the steady-state rate constant for ADP incorporation at site 1 (2 s^{-1} at 120 μM CaATP) is significantly larger than the initial exchange rate constant (0.1 s^{-1}). Also, the steady-state exchange rate constant is comparable to the catalytic rate constant (3.2 s^{-1}). Although this has been proposed on the basis of less direct measurements (Wu & Boyer, 1986), this appears to be the first instance where a measurement of the rate constant for nucleotide incorporation has been made during steady-state catalysis. At this time, all that can be stated is that the steady-state rate constant and the catalytic rate constant are comparable (within a factor of $\sim$2). A more quantitative comparison is not possible due to the low precision of the measurements and the difficulty in assessing what fraction of the enzyme population is involved in the process.

The role of site 2 is still not understood. Tightly bound MgATP at site 2 is not hydrolyzed during catalysis, eliminating this site as a possible catalytic site. In addition, occupation by MgATP does not affect the exchange rate at site 1 or the catalytic rate nor does it influence the inhibitory effects of CaADP during steady-state hydrolysis. Consequently, this site does not have a known regulatory function. However, since this site is always partially occupied during catalysis, it may still play some unknown regulatory role.

The results obtained are consistent with both site 1 and site 3 serving as catalytic sites. The possibility of additional lower affinity sites participating in catalysis cannot be excluded. However, no evidence exists to support such a hypothesis. The sigmoidal dependence of β on the concentration of CaATP (Figure 5), earlier steady-state kinetics (Bruist & Hammes, 1982), and O–P exchange experiments [cf. Kohlbrenner and Boyer (1983)] are indicative of a complex mechanism for catalysis. One mechanism that has been proposed is the "binding change mechanism" [cf. Hackney et al. (1979)] in which the catalytic activity occurs alternately at different sites, with product release at one catalytic site triggered by substrate binding at a different catalytic site. However, other mechanisms also are possible. For example, a steady-state mechanism involving two-site positive cooperativity in substrate binding, with different catalytic rates when one or two sites are occupied, also is consistent with the data. A third mechanism often invoked to describe the kinetic behavior of ion pumping coupled to enzyme catalysis (de Meis & Vianna, 1979; Cantley, 1981; Jencks, 1980; Hammes, 1982) involves parallel pathways for catalysis. The enzyme is assumed to exist in two different conformations, both capable of catalyzing hydrolysis. Even with a single catalytic site, such a mechanism can display apparent positive cooperativity in the steady state [cf. Koland and Hammes (1986)]. Cooperativity among multiple substrate binding sites can be added to this mechanism as well. In the three mechanisms discussed, the steady-state rate laws can display apparent positive cooperativity. At low substrate concentrations, the rate law reduces to

$$\beta = A_0[\text{CaATP}] + B_0[\text{CaATP}]^2 \quad (9)$$

The solid line in Figure 5 is the best fit to eq 9 with $A_0 = (3.0 \pm 0.4) \times 10^{-3}\ \mu M^{-1}\ s^{-1}$ and $B_0 = (3.1 \pm 0.5) \times 10^{-4}\ \mu M^{-2}\ s^{-1}$. More extensive steady-state data (Bruist & Hammes, 1982) and the dependence of the O–P exchange rate on substrate concentration are consistent with all three types of mechanisms discussed.

Currently, a distinction cannot be made between the mechanisms presented. The binding change mechanism requires that the sites be catalytically equivalent, whereas the other two do not. The catalytic sites clearly are not structurally equivalent with respect to the γ, δ, and ϵ subunits [cf. Richter et al. (1985)], but the relevance of this structural inequivalence to enzyme catalysis has not been established.

ACKNOWLEDGMENTS

We are indebted to Lisa Bosch for preparation of the enzyme.

Registry No. ATPase, 9000-83-3; CaATP, 15866-84-9; MgATP, 1476-84-2.

REFERENCES

Avron, M. (1960) *Biochim. Biophys. Acta 40*, 257–272.
Bar-Zvi, D., & Shavit, N. (1982) *Biochim. Biophys. Acta 681*, 451–458.
Binder, A., Jagendorf, A., & Ngo, E. (1978) *J. Biol. Chem. 253*, 3094–3100.
Bock, R. M., Ling, N.-S., Morell, S. A., & Lipton, S. H. (1956) *Arch. Biochem. Biophys. 62*, 253–264.
Bruist, M. F., & Hammes, G. G. (1981) *Biochemistry 20*, 6298–6305.
Bruist, M. F., & Hammes, G. G. (1982) *Biochemistry 21*, 3370–3377.
Cantley, L. C. (1981) *Curr. Top. Bioenerg. 11*, 201–237.
Carlier, M. F., & Hammes, G. G. (1979) *Biochemistry 18*, 3446–3451.
Carmelli, C. (1979) in *Cation Flux Across Biomembranes* (Carafoli, E., & Mukohata, Y., Eds.) pp 249–259, Academic Press, New York.
Cash, D. J., & Hess, G. P. (1981) *Anal. Biochem. 112*, 39–51.
Cerione, R. A., & Hammes, G. G. (1982) *Biochemistry 21*, 745–752.
Cognet, J. A., & Hammes, G. G. (1983) *Biochemistry 22*, 3002–3007.
deMeis, L., & Vianna, A. L. (1979) *Annu. Rev. Biochem. 48*, 275–292.
Farron, F., & Racker, E. (1970) *Biochemistry 9*, 3829–3836.
Feldman, R. I., & Sigman, D. S. (1982) *J. Biol. Chem. 257*, 1676–1683.
Hackney, D. D., Rosen, G., & Boyer, P. D. (1979) *Proc. Natl. Acad. Sci. U.S.A. 76*, 3646–3650.
Hammes, G. G. (1982) *Proc. Natl. Acad. Sci. U.S.A. 79*, 6881–6884.
Harris, D. A., & Slater, E. C. (1975) *Biochim. Biophys. Acta 387*, 335–348.
Jencks, W. P. (1980) *Adv. Enzymol. Relat. Areas Mol. Biol. 51*, 75–106.
Khan, M. M. T., & Martell, A. E. (1962) *J. Phys. Chem. 76*, 10–15.
Kohlbrenner, W. E., & Boyer, P. D. (1983) *J. Biol. Chem. 258*, 10881–10886.
Koland, J. G., & Hammes, G. G. (1986) *J. Biol. Chem. 261*, 5936–5942.

Lien, S., & Racker, E. (1971) *Methods Enzymol. 23*, 547-555.
McCarty, R. E., & Moroney, J. E. (1985) in *The Enzymes of Biological Membranes* (Martonosi, A. N., Ed.) 2nd ed., Vol. 4, pp 383-413, Plenum Press, New York.
Moroney, J. V., Lopresti, L., McEwen, B. F., McCarty, R. E., & Hammes, G. G. (1983) *FEBS Lett. 158*, 58-62.
Penefsky, H. S. (1977) *J. Biol. Chem. 252*, 2891-2899.
Richter, M. L., Snyder, B., McCarty, R. E., & Hammes, G. G. (1985) *Biochemistry 24*, 5755-5763.
Schinkel, J. E., & Hammes, G. G. (1986) *Biochemistry 25*, 4066-4071.
Schumann, J., & Strotmann, H. (1981) in *Photosynthesis II. Electron Transport and Photophosphorylation* (Akoyunoglou, G., Ed.) pp 881-892, Balaban International Science Services, Philadelphia, PA.
Shahak, Y. (1986) *Eur. J. Biochem. 154*, 179-185.
Strotmann, H., & Bickel-Sandkötter, S. (1977) *Biochim. Biophys. Acta 460*, 126-135.
Wu, D., & Boyer, P. D. (1986) *Biochemistry 25*, 3390-3396.

Low-Temperature Electron Paramagnetic Resonance Study of the Ferricytochrome *c*-Cardiolipin Complex

James S. Vincent
Department of Chemistry, University of Maryland Baltimore County, Catonsville, Maryland 21228
Hideo Kon and Ira W. Levin*
Laboratory of Chemical Physics, National Institute of Diabetes and Digestive and Kidney Diseases, National Institutes of Health, Bethesda, Maryland 20892
Received October 10, 1986; Revised Manuscript Received December 11, 1986

ABSTRACT: The electron paramagnetic resonance spectrum of the ferricytochrome *c* complex with cardiolipin was observed at temperatures below 20 K. For the low-spin iron(III) heme system complexed with the negatively charged lipid, the tetragonal and rhombic ligand field parameters ($\Delta/\lambda = 3.58$, $V/\lambda = 1.82$) differ significantly from those ($\Delta/\lambda = 2.53$, $V/\lambda = 1.49$) of the free ferricytochrome *c* sample. The *g* values of the complex ($g_x = 1.54 \pm 0.02$, $g_y = 2.26 \pm 0.01$, $g_z = 3.02 \pm 0.01$) are compared to the values for free ferricytochrome *c* ($g_x = 1.25 \pm 0.02$, $g_y = 2.25 \pm 0.01$, $g_z = 3.04 \pm 0.01$). Spectral alterations are interpreted in terms of the ligand field changes induced within the heme group by association with the negatively charged phosphoglyceride.

Interest in cytochrome *c* interactions with either zwitterionic or charged lipid assemblies stems primarily from attempts to characterize physically the perturbations to membrane structure arising from the binding of extrinsic bilayer proteins (Devaux et al., 1986; DeKruijff et al., 1980; Brown & Wüthrich, 1977). Since cytochrome *c* may interact selectively with cardiolipin in the inner mitochondrial membrane, the properties of this particular model system become important both in assessing putative configurational changes in either the protein or the lipid component of the complex and in assigning functional significance to the structural reorganizations that occur during binding (Vincent & Levin, 1986; DeKruijff & Cullis, 1980). In particular, ferricytochrome *c* in complex form with cardiolipin exhibits considerably different properties from those of the free protein. For example, the redox potential is decreased by approximately 40 mV (Kimelberg & Lee, 1970), and although the visible spectra shift slightly, the spectral patterns remain characteristic of the oxidized species (Vincent & Levin, 1986). In addition, the resonance Raman spectrum of the ferricytochrome *c*-cardiolipin complex reflects the vibrational frequency and intensity markers of the reduced iron species even though the iron oxidation state remains unaffected (Vincent & Levin, 1986). That is, on complexation, the periphery of the porphyrin groups assumes the reduced cytochrome *c* conformation without the presence of a chemical reductant. As part of the latter resonance Raman study, the electron paramagnetic resonance (EPR) spectrum of the ferricytochrome *c* complex was measured at 77 K in order to confirm the existence of the low-spin Fe(III) species (Vincent & Levin, 1986). Since the EPR spectra of the ferricytochrome *c* complex with cardiolipin reflect modifications in the heme structure of uncomplexed cytochrome *c*, we discuss here the perturbed EPR spectra of the associated species, determined at temperatures below 20 K, in terms of the induced ligand field changes.

Experimental Procedures

Ferricytochrome *c*, obtained from Sigma (horse heart VI), was purified by chromatography according to the procedure of Brautigan et al. (1978). The 695-nm transition was clearly observable; the visible spectra of the reduced species were identical before and after treatment with carbon monoxide (Theorell & Akerson, 1941), indicating that the heme group remained fully coordinated with protein ligands (George & Schejter, 1964). Cardiolipin (bovine heart) was obtained from Avanti Polar Lipids and used without further purification.

The EPR spectra were collected with a Varian Century-100 X-band spectrometer. The sample was cooled with helium gas conducted from a liquid helium Dewar by an Air Products and Chemicals Heli-Tran transfer line. The temperature for each experiment was determined by using a germanium resister and maintained during each experiment at a constant temperature between 7 and 20 K. The magnetic field intensity was monitored by counting the frequency of the proton nuclear magnetic resonance; the microwave frequency was calibrated with a cavity wavemeter.